

Quantum-Inspired Computing: Can it be a Microscopic Computing Model of the Brain?

Yasunao Katayama

IBM Research - Tokyo

email: yasunaok@jp.ibm.com

Abstract: Quantum computing and the workings of the brain have many aspects in common and have been attracting increasing attention in academia and industry. The computation in both is parallel and non-discrete. Though the underlying physical dynamics (e.g., equation of motion) may be deterministic, the observed or interpreted outcomes are often probabilistic. Consequently, various investigations have been undertaken to understand and reproduce the brain on the basis of quantum physics and computing ¹⁻⁹. However, there have been arguments on whether the brain can and have to take advantage of quantum phenomena that need to survive in the macroscopic space-time region at room temperature ¹⁰⁻¹². This paper presents a unique microscopic computational model for the brain based on an ansatz that the brain computes in a manner similar to quantum computing, but with classical waves. Log-scale encoding of information ¹³ in the context of computing with waves ¹⁴ is shown to play a critical role in bridging the computing models with classical and quantum waves. Our quantum-inspired computing model opens up a possibility of unifying the computing framework of artificial intelligence and quantum computing beyond quantum machine learning approaches.

arXiv:1904.10508v2 [q-bio.NC] 13 Nov 2019

Contents

| | | |
|----------|--|-----------|
| 1 | Introduction | 3 |
| 2 | Encoding cubits into classical waves | 5 |
| 3 | Operations for cubits | 9 |
| 4 | Log-scale encoding to bridge QC and QIC | 10 |
| 5 | Discussion | 14 |
| 6 | Conclusion | 17 |

1 Introduction

Artificial intelligence (AI) and quantum computing (QC) are two rapidly evolving technologies that are redefining computing. The capability of computers to handle narrowly defined AI tasks is surpassing human capability, and the research focus is shifting toward giving computers broader and more general AI capabilities¹⁶. Quantum computers are expected to solve certain types of problems that conventional computers are hard to solve¹⁷. Since QC and the workings of the brain share many aspects in common, it is not surprising to see that there have been various research activities aimed at understanding the computing model of the brain on the basis of quantum physics and QC as early as the 1970s²⁻⁶. As a result of rapid advancement of QC, quantum machine learning has been attracting a lot of attention in both AI and QC research communities⁷⁻⁹. Indeed, the computation in both cases is executed in parallel with non-discrete variables. Though the underlying physical dynamics (e.g., equation of motion) may be deterministic, the observed or interpreted outcomes are more probabilistic.

However, at the same time there have been controversial arguments from physics (i.e., material) and cognitive science (i.e., mental) points of view on whether the brain, both biological and artificial, can and have to take advantage of quantum features, such as Tensor-product statespace and entanglement, that need to survive in macroscopic space-time regions at room temperature¹⁰⁻¹². Though macroscopic quantum phenomena are increasingly being observed in the lab^{18,19}, they are seldom perceived in ordinary life. In addition, from a computing point of view, though there is much less doubt on inherent QC advantages in quantum information processing^{20,21}, AI

workloads in general process huge data sets and irreversible algorithms with noise in computing environment and data, which may not always be effectively translated into tensor product entangled statespaces with a limited number of qubits and their interconnects. In other words, the statespace advantage of QC may quickly diminish unless the symmetry of the problem cleanly fit to exponentially-large Hilbert state spaces with exclusively linear operators on them. QC-unique constraints such as no cloning, strict reversibility, measurement complications, may pose additional challenges in application coverage, system scalability, and fault and error tolerances, if we dare to pursue strict QC approaches universally for classical and data-intensive computing problems of AI workloads. On the other hand, parallel and non-discrete dynamics is not unique to quantum physics but is something natively observed in ordinary classical physics, such as wave dynamics

14.

Here in this paper, we propose quantum-inspired computing (QIC) as energy and computationally efficient microscopic computing model for classical workloads, in particular AI. As shown in Fig. 1, our approach is unique compared with existing QC-based approaches, since quantum physics is not prerequisite in the computing model. Instead, parallel computing advantage of QC is incorporated in a more general natural computing context with less QC-unique constraints. More specifically, our model is based in as a network of elastic wave processing of spikes. Wave superposition and thresholding can smoothly and precisely execute, without being influenced by collision and congestion, weighted sum and ReLU operations, which are key arithmetic in modern AI processing. Our quantum-inspired modeling approach with natively incorporating precise spike correlations in continuous time allows for the temporal computing more rigorously based on origi-

nal spiking neural network (SNN) model ²² and should differentiate it from existing neuromorphic approaches ^{23–25}. In order for physically directive and nonblocking wave nature to prevail at a small scale for energy efficiency and integration, it is essential to reduce the wavelength by reducing the spike signal velocity ¹⁴. Quantum-inspired approach has been improving classical counterpart at different levels ¹⁵. The present work is quantum-inspired approach at a microscopic computing level.

2 Encoding qubits into classical waves

The wave nature of matters and fields plays a critical role in both classical and quantum physics. In classical physics, a wave is a phenomenon that can elastically transfer energy and information, without transporting matter, via the interplay between displacement and a linearly responsive restoring force, such as between a displacement current and an electrical and magnetic field in the case of electromagnetic waves. Waves carry electrical signals, not electrons. In quantum physics, a wave function is an essential means to describe quantum phenomena in both ground and excited states. Though classical waves do not exhibit quantum-mechanical coherence, such as macroscopically observed in lasers and superconductors, they have their own wave characteristics such as superposition and interference. Classically coherent waves can be generated by externally exciting the system in phase with forced vibrations. Such classical waves are in accordance with classical dynamics with commutable variables and contiguous energy spectra. Interestingly, the coherence of such macroscopic classical waves can often last for a substantial amount of time even at room temperature, as observed in radio waves in wireless communication or sound waves in a music

hall.

In this paper, we will construct a computing model with classical waves. Let us start the discussion on how to take advantage of the classical wave features in computing by defining, in analogy to the qubit in quantum computing, the cubit, which is an abbreviation of *classical universal bit*. The notation used for cubits is similar to the standard Dirac notation for qubits but with double bras and kets. Let $||0\rangle\rangle$ and $||1\rangle\rangle$ be normalized orthogonal basis vectors for cubits:

$$\langle\langle 0|0\rangle\rangle = \langle\langle 1|1\rangle\rangle = 1, \quad (1)$$

$$\langle\langle 0|1\rangle\rangle = \langle\langle 1|0\rangle\rangle = 0. \quad (2)$$

The scalar product is defined as a conjugate integral in a predefined volume V , which can be flying or standing as discussed later. States with higher indices and harmonics for cubits can be considered similar to qubits²⁶, but we will not go further for simpler comparison. Using

$$\langle\langle x_1|x_2\rangle\rangle = \delta(x_1 - x_2) \quad (3)$$

enables the actual waveform in space time to be given as

$$f_0(x) = \langle\langle x|0\rangle\rangle, \quad (4)$$

$$f_1(x) = \langle\langle x|1\rangle\rangle. \quad (5)$$

Therefore, the scalar product can be expressed as an integral in space coordinates:

$$\langle\langle 0|1\rangle\rangle = \int_{x \in V} f_0^*(x) f_1(x) dx. \quad (6)$$

The difference between bra or ket may not matter much if the waves are defined in \mathbb{R} . Complex conjugate $*$ should be used when dealing with complex numbers. An arbitrary cubit state

$$||a\rangle\rangle = \bar{a} ||0\rangle\rangle + a ||1\rangle\rangle \quad (7)$$

can have a wave form in space time as

$$a(x) = \bar{a}f_0 + af_1. \quad (8)$$

Cubits can be flying or standing depends on whether the basis vector $||0\rangle\rangle$ and $||1\rangle\rangle$ and the associated volume V is flying or standing. The difference in the mathematical formulation is not as large as that in the implementation, given that it is only a matter of which coordinate to select, as illustrated in Fig. 2. In other words, when a flying cubit and associated V are moving at a constant velocity v ideally with little dispersion, the flying cubit can be considered standing when viewed from the coordinate attached to it. Assuming $v \ll c$ (i.e., nonrelativistic) with no dispersion, an arbitrary flying cubit state $||a(x, t)\rangle\rangle_f$ can be related to a standing one $||a(x, t)\rangle\rangle_s$ as

$$||a(x, t)\rangle\rangle_f = \int ||a(x - x', t)\rangle\rangle_s \delta(x' - vt) dx'. \quad (9)$$

The use of slow v is essential to exploit wave nature with energy efficiency and integration ¹⁴. In QC systems, qubits are often standing. Flying qubits are diffusive except for massless qubits, i.e., those flying at the speed of light. On the other hand, spikes in the brain are more consistent with flying cubit picture. Encoding information into standing cubits may be related to digital recording techniques, such as partial response maximum likelihood (PRML) encoding ²⁷. While those techniques are considered as taking advantage of standing wave nature of recording signals

with the finite frequency response of the media *for memory and storage*, the brain is considered as using flying wave nature of spike signals *for computing* in the present model.

There are multiple types of logical cubits:

Normalized full cubit $||a\rangle\rangle := \bar{a} ||0\rangle\rangle + a ||1\rangle\rangle, |\bar{a}|^2 + |a|^2 = 1 \in U(1) \text{ or } SO(2)$

Normalized half cubit $||a\rangle\rangle := a ||1\rangle\rangle, 0 \leq |a|^2 \leq 1 \in U(1) \cap \mathbb{R}$

Unnormalized full cubit $||a\rangle\rangle := \bar{a} ||0\rangle\rangle + a ||1\rangle\rangle \in \mathbb{R}^2 \text{ or } \mathbb{C}$

Unnormalized half cubit. $||a\rangle\rangle := a ||1\rangle\rangle \in \mathbb{R}$

Cubits are defined not in the Bloch sphere ($SU(2)$ or $SO(3)$) like qubits. The $||0\rangle\rangle$ amplitude for the half cubits is implicit and may result in more efficient gate implementation if $||0\rangle\rangle$ can be regarded as the ground state (i.e., no excitation).

There are several ways to encode logical cubits into physical waves. Specific examples are shown in Figs. 2 (a)–(d). Examples (a) and (c) are for half cubits, and examples (b) and (d) are for full cubits. Examples (a)–(c) are with single wires, while example (d) is with a spatially distinguishable wire pair. In other words, examples (a)–(c) require a single lane per cubit, while example (d) requires dual-rail encoding, i.e., two physical lanes to encode a single logical cubit. The unnormalized half qubit could be ill defined without dual rail coding, since the amplitude of $||0\rangle\rangle$ cannot be estimated from that of $||1\rangle\rangle$. Example (b) is identical to phase shift keying in wireless communication, which is typical with a carrier. Example (a) can be considered as the real part of example (b) though (a) can be encoded without the carrier as well. Logical information can be encoded into multiple physical cubits by using majority logic coding, such as rate or population

coding, or by using temporal interval coding on a continuous non-discrete time scale.

Note that the present cubit formulation is mostly for computing, not for physics. We inherited the standard bra and ket notation from quantum physics to describe cubits in a consistent manner with qubits. If we dare to approximately relate cubit states to boson qubit ensemble states by taking the classical limit of the occupation numbers for $|0\rangle$ and $|1\rangle$, i.e., $n_0, n_1 \rightarrow \infty$, and by neglecting the off-diagonal terms, we get

$$||0\rangle\rangle \sim \sqrt{\langle n_0 \rangle}, \quad (10)$$

$$||1\rangle\rangle \sim \sqrt{\langle n_1 \rangle}. \quad (11)$$

Therefore, cubits may be regarded as population coded qubits in ensemble average. This relation is to be revisited later for both bosons and fermions.

3 Operations for cubits

QIC can have various gate primitives for linear and nonlinear operations. Linear operations are natural outcomes of wave superpositions, and the corresponding primitives are coupler with full cubits for reversible operations, and adder or combiner (and coupler with half cubits) for irreversible operations, respectively. Splitter is the reverse operation of combiner. The fixed multiplier with the constant W for unnormalized cubits has to be either lossy ($|W| < 1$) or active ($|W| > 1$). Nonlinear operations such as wave multiplication are also possible. These operations for classical waves may look familiar to those with wireless communication backgrounds since they are typically used for splitting and combining, and for up- and down-conversion of wireless signals.

Integrate and fire operation makes discrete binary decisions of either fire $||1\rangle\rangle$ or not fire $||0\rangle\rangle$ for normalized half qubit out of non-discrete continuous states $||a\rangle\rangle$.

Figure 3 compares linear and nonlinear operations for single- and multiple-input gates with bits, cubits, and qubits in classical, wave-based, and quantum computing. The mathematical space corresponding to the number system of choice for each basic unit is represented by T . For example, $T = SU(2)$ for qubits. For classical computing, NOT and XOR gates perform linear operations over Cartesian product states $T \oplus T$ while AND and OR gates perform nonlinear operations. Fredkin or Toffoli gates are listed as classical reversible gates²⁸. The most general form of a nonlinear operation can be represented as a memory, for which any output can be defined at the expense of 2^N resources for N address inputs. QC gates perform linear operations in $SU(2)$ or in its tensor product space, $T \otimes T$. The measurements nonlinearly reduce qubits in the tensor product states to ordinary bits in the Cartesian product states, though they are still projective linear operations in the original tensor product states, but nonlinearity can arise if multiple qubit measurement results are reduced in Cartesian product states. Measurements in QC can be related to integrated and fire in QIC as a decision process of superposed states to one of the orthogonal states.

4 Log-scale encoding to bridge QC and QIC

Let us consider a decision problem with each decision represented by a qubit: $p_i = |\langle 1|p_i\rangle|^2$ and $\bar{p}_i = 1 - p_i = |\langle 0|p_i\rangle|^2$. In other words,

$$|\mathbf{In}_i\rangle = |p_i\rangle = \bar{p}_i |0\rangle + p |1\rangle. \quad (12)$$

When the state consists of a tensor product state of independent (i.e., no entanglement) qubit states as $|p_0\rangle \otimes |p_1\rangle \otimes \dots \otimes |p_n\rangle$, the probability $P_{\{d_1 \dots d_n\}}$ of having a decision $\{d_1 \dots d_n\}$ with $d_i = 0$ or 1 is

$$P_{\{d_1 \dots d_n\}} = \prod_{j=1}^n |\langle 1|p_j\rangle^{d_j} \langle 0|p_j\rangle^{1-d_j}|^2. \quad (13)$$

When we take the log of both sides,

$$\log P_{\{d_1 \dots d_n\}} = 2 \sum_{j=1}^n \log |\langle 1|p_j\rangle^{d_j} \langle 0|p_j\rangle^{1-d_j}|. \quad (14)$$

When w_{ij} identical qubits are involved in decision P_i , the equations become

$$P_{i\{d_1 \dots d_n\}} = \prod_{j=1}^n |\langle 1|p_j\rangle^{d_j} \langle 0|p_j\rangle^{1-d_j}|^{2w_{ij}}. \quad (15)$$

and

$$\log P_{i\{d_1 \dots d_n\}} = 2 \sum_{j=1}^n w_{ij} \log |\langle 1|p_j\rangle^{d_j} \langle 0|p_j\rangle^{1-d_j}|. \quad (16)$$

Note that no cloning theorem does not allow the duplication for arbitrary qubit states.

The following log relationship can translate Tensor-product qubit to Cartesian-product cubit as:

$$\langle\langle 1|\text{Out}_i\rangle\rangle \sim \log P_{i\{d_1 \dots d_n\}}, \quad (17)$$

$$\langle\langle d_i|\text{In}_i\rangle\rangle \sim \log |\langle 1|p_i\rangle^{d_i} \langle 0|p_i\rangle^{1-d_i}|. \quad (18)$$

In other words, the probability in a cubit are interpreted as a log scale encoding of the probability in a qubit. Log-scale encoding is a standard technique in probability calculations, such as used in log likelihood estimations. It simplifies probability calculations for a wide dynamic range inputs and

seems consistent with that fact that the biological brain can compute with a wide dynamic range of sensory signals ²⁹. The encoding with excitatory and inhibitory neurons for p and \bar{p} in a dual-rail manner is possible. The log scaling encoding can also provide a natural rectifying capability with appropriate biasing b_i as

$$\langle\langle 1|\text{Out}_i\rangle\rangle = 2 \sum_{j=1}^n w_{ij} \langle\langle d_j|\text{In}_j\rangle\rangle + b_i. \quad (19)$$

When the probabilities are normalized per unit time interval, they corresponds to the spike rate which is the inverse of the time-to-spike interval ³⁰. The neuron dynamics in this model is driven by the digital number of replicated spike paths rather than the analog strength of each spike and its synaptic weight. The log-scale encoding can significantly reduce the number of spikes for a given signal dynamic range. When cubits are flying, Eq.19 can be expressed, by using Eq. 9, as

$$|\langle\langle \text{Out}_i(t)\rangle\rangle = \int \sum_j W_{ij}(t') |\langle\langle \text{In}_j(t-t')\rangle\rangle dt' + b_i, \quad (20)$$

by substituting $W_{ij}(t) = 2w_{ij}\delta(t - d_{ij})$, where d_{ij} is the delay between node i and j and is related to the path length L_{ij} by $d_{ij} = L_{ij}/v$.

Comparison of cubit and qubit operations for a binary neuron as an example is shown in Fig. 4. Probabilities of cubits and qubits for a binary neuron can be inter-related by log encoding. The present model describes inferencing. Eventually, weight update rules for learning has to be worked out, ideally based on direct temporal correlations of spikes (i.e., cubits) rather than indirect formulations based on rate coding ^{31,32}.

QIC can become a superior one for non-quantum applications, so should not always be considered as an inferior version of QC. Indeed, the approach is aiming at expanding the applica-

tion coverage of QC-like computing by appropriately loosened constraints of QC without much affecting its advantages. This quantum-inspired approach can be interpreted as depth=1 noisy intermediate-scale quantum computing (NISQ) ³³ with ensembles of flying qubit inputs as spikes in density matrices. QIC for neural operations interpreted as ensembles of parallel and concurrent QC operations is shown in Fig. 4 (a). It can support nonbinary weights by the qubit inputs as ensembles of concurrent and parallel qubit inputs:

$$||\text{In}\rangle\rangle \langle\langle \text{In}|| \sim n_{trial}(\bar{p}|0\rangle\langle 0| + p|1\rangle\langle 1|). \quad (21)$$

A calculated result for ensembles as a function of n_{trial} is shown in Fig. 4 (b). Each trial consists of ten parallel qubit measurements. The variance is expected to converge as $\sim 1/\sqrt{n_{trial}}$ for qubits by concurrently executing entire trials in parallel. This concurrent and parallel trial is valid for both bosons and fermions, and we can write as

$$n_0 = n_{trial}\bar{p}, \quad (22)$$

$$n_1 = n_{trial}p. \quad (23)$$

As summarized in Fig. 4 (c) QIC distinguish itself from classical computing in terms of parallel execution and superposed states and from QC in terms of log-scale encoding and concurrent execution. Since qubits are classical consisting of ensembles of orthogonal qubits, they can be duplicated to constitute nonbinary weights without being constrained by the no cloning theorem. Concurrent ensembles of try and measure executions can significantly accelerate and scale a wide range of less entangled AI workloads without QC-unique constraints even under noises in data and environment. Thus, the present QIC approach has a good potential to deliver much better throughput and scalability for the main-stream AI workloads than strict QC counterpart.

When these primitives are combined, neuron models to describe an abstract level PHY can be constructed, as exemplified in Fig. 4 (a). It consists of wave processes in continuous time model. The output activation is triggered by input correlations, not input-output (scattering model). It can accept both excitatory and inhibitory inputs. Weight matrix is expressed by Fredkin gate as a coupler with weight adjustment, details of which are described in Appendix A. Fredkin gate can output the leftover wave energy from the other port. This otherwise wasted wave energy would be useful for weight update with learning. Simulation results is shown in Fig. 4 (b) using a neural channel and circuit modeling technique discussed in another paper^{34,35}. When the leakage parameter of integrate and fire block is appropriately set, spike temporal correlations can be extracted by appropriately adjusting the leakage time constant of the membrane potential. When $\Delta d = d_{i+1} - d_i = 200$ ps (upper), spikes from multiple inputs are less temporally correlated, and thus output does not fire. When $\Delta d = 100$ ps (lower), spikes are more temporally correlated and output fires.

5 Discussion

We have shown that computing with cubits can be performed in parallel by using superposed states, similar to qubits. Thus, here we address the differences between QC and QIC, starting with the advantages of QIC for classical computing tasks. In short, cubits are better fit for accelerating general classical algorithms. Using cubits can avoid the complications associated with reversibility, cloning, and measurement. This is important given that many real-world algorithms (e.g., those for AI tasks) are not reversible and require copying of data. In addition, there is less overhead for data IO when using cubits since information in classical domain does not have to be

converted into information in quantum domain in Tensor-product states with a smaller number of qubits. The dephasing time for classical waves is often much longer even at room temperature, which is also the case for spike signals in the biological brain. The use of cubits thus offers the potential for deeper circuits with less error correction overhead. In contrast, QIC is not suitable for quantum information processing. No exponential tensor-product linear state spaces are natively available, and nonlocal entanglement features are missing. Even though both cubits and qubits can be reduced to the same classical bit operations, they behave differently in their own mathematical spaces. This makes it fundamentally difficult to use cubits to emulate qubits for quantum information processing. The following arguments in Appendix B may provide a better understanding of this situation by illustrating the extent to which cubits can be used to perform algorithms involving entanglement. More rigorous formulation of QIC may provide a new perspective on computational complexity arguments ³⁶.

Our approach is not as extreme as reversible computing ³⁷ in terms of energy per computation limit, since it allows for and asks for dissipatively losing non-essential information. Thus, it can alleviate logical complications associated with stringent reversible computing constraints and more suitable for inherently irreversible AI workloads. We exploit elastic waves rather than matters (i.e., not billiard balls) as information carrier for stable solid-state implementation. The use of orders of magnitude slower waves than the speed of light is essential for energy efficiency and integration. Our conjecture is that this is what the biological brain has already taken advantage of with spike signals for energy efficiency.

Compared with existing neuromorphic computing approaches, our approach can better incorporate time as a resource for computation and communication, which is considered essential for SNNs²². Otherwise, though spike signaling can improve tolerance to noise and disturbance including baseline wander, simple rate coded spiking neural networks would result in exponentially less efficient than binary coded analog neural networks in terms of coding efficiency in neural channels³⁵. Thus, though many prior art neuromorphic research results claim energy efficiency, in reality the total power reduction would be limited when spiking IOs are inefficiently coded. We expect that, in addition to coding efficiency, supporting temporal coding, such as interpulse-interval coding³⁸, natively in continuous time with desired stochasticity without being affected by undesired temporal jitters due to signal collision and congestion can provide a new perspective. Importance of temporal delay in biological brains has also addressed in neuroscience³⁹.

The proposed QIC should not be considered the same as standard analog signal processing. The underlying physical processes are quite distinctive. The former is elastic and nondissipative while the latter is often inelastic and dissipative. In other words, the signal is represented by nonequibrated wave dynamics, rather than equilibrated potential. It can be considered as a miniaturized version of computing with radio frequency (RF) passives, exploiting wave-based signal processing features, such as superposition, naturally without signal collision nor unwanted leakage. Signals are physically and logically directive and nonblocking to each other thanks to the wave nature. As was mentioned earlier, it is essential to reduce the wavelength of the spike signal with respect to the transmission length by reducing the spike signal velocity. This aspect has not been addressed much in conventional analog neuron models.

QIC can become a fair candidate for the microscopic computing model for the artificial brain, in particular considering to realize SNNs with a good temporal degrees of freedom. It also provides a new perspective on the microscopic computing model for the biological brain whether quantum effects are mandatory to explain brain computing functionalities, in addition to quantum effects in biochemistry perspectives. From the computing model point of view, entanglement aspects would be a key to identify whether quantum effects are mandatory in order to explain brain functionalities. Further arguments on entanglement with QIC is given in Appendix B.

6 Conclusion

We proposed quantum-inspired computing as energy- and computationally-efficient microscopic computing model for AI workloads in analogy to quantum computing. Parallel computing advantage with superposed states will be incorporated in a more general natural computing context with less constraints. Log-scale encoding of information is shown to play a critical role in bridging the computing models of classical and quantum waves. Our goal is to redefine AI computing model with quantum-inspired approach and ultimately unify the computing model of AI and QC, hoping that this path will bring us to better understand the microscopic computing model of the brain.

Appendix A: Implementation sketch

There are various candidates to implement cubits and their operations, such as spin waves, acoustic waves, slow optics, and ion density waves. Here, we show implementation sketch for key primitive building blocks using nanostructured electronics in Fig. 6. It may have a better path to be migrated

in existing semiconductor technologies, since no signal wave conversion is needed. The purpose is to show that the proposed computing model has a reasonable path toward implementation, but further study is needed to identify the most suitable way of realizing the device. In Fig. 6 (a), weight matrix diagram is represented by Fredkin gate for cubits. It has three inputs:

$$||c\rangle\rangle = \bar{c} ||0\rangle\rangle + c ||1\rangle\rangle, \quad (24)$$

$$||p\rangle\rangle = \bar{p} ||0\rangle\rangle + p ||1\rangle\rangle, \quad (25)$$

$$||c\rangle\rangle = \bar{q} ||0\rangle\rangle + q ||1\rangle\rangle \quad (26)$$

for full cubits and

$$||c\rangle\rangle = c ||1\rangle\rangle, \quad (27)$$

$$||p\rangle\rangle = p ||1\rangle\rangle, \quad (28)$$

$$||c\rangle\rangle = q ||1\rangle\rangle \quad (29)$$

for half cubits. Note that $||c\rangle\rangle$ signal may not be spiking. The outputs are defined as

$$||c\rangle\rangle = \bar{c} ||0\rangle\rangle + c ||1\rangle\rangle, \quad (30)$$

$$\bar{c} ||p\rangle\rangle + c ||q\rangle\rangle = (\bar{c}\bar{p} + c\bar{q}) ||0\rangle\rangle + (\bar{c}p + cq) ||1\rangle\rangle, \quad (31)$$

$$\bar{c} ||q\rangle\rangle + c ||p\rangle\rangle = (\bar{c}\bar{q} + c\bar{p}) ||0\rangle\rangle + (\bar{c}q + cp) ||1\rangle\rangle \quad (32)$$

for full cubits and

$$||c\rangle\rangle = c ||1\rangle\rangle, \quad (33)$$

$$\bar{c} ||p\rangle\rangle + c ||q\rangle\rangle = (\bar{c}p + cq) ||1\rangle\rangle, \quad (34)$$

$$\bar{c}||q\rangle\rangle + c||p\rangle\rangle = (\bar{c}q + cp) ||1\rangle\rangle \quad (35)$$

for half cubits. As indicated in these equations, both superposition (addition) and multiplications are involved in the cubit Fredkin gate. The Fredkin gate is a universal classical gate with constant ancilla inputs²⁸. Fredkin gate is more suitable than Toffoli gate for our purpose since the number of conserved 0's and 1's between inputs and outputs can lead to more efficient passive gate implementations for better energy efficiency. Normalized half cubits with $||0\rangle\rangle$ for no signal and $||1\rangle\rangle$ for a full signal can be assumed. With this assumption, superposed cubit states can be represented by the scalar strength of $||1\rangle\rangle$. Because the Fredkin gate conserves the number of 0's and 1's, the gate can be implemented passive wave couplers without active amplification. With an active amplification option, the gate can generate signal gain for a larger fanout assuming unnormalized cubits. When Fredkin gates are combined, the weighted sums of any number of inputs and outputs can be flexibly calculated by using analog weighted-sum calculation. The data cubits $||p\rangle\rangle$ and $||q\rangle\rangle$ for the Fredkin gate are repartitioned in accordance with instructions from the control cubit $||c\rangle\rangle$. When the blocks of the gate structure are combined, they can represent any repartitioning across a large number of data cubits as a unitary (flux conserving) transformation.

Figure 6 (b) depicts Fredkin gate with delay for cubits with nanostructured electron wave guides and utilizes lateral tunneling transistor structure⁴⁰⁻⁴², with energy diagram for lateral tunneling transistor in Fig. 6 (c). Here, single-particle electron quantum wave functions are treated as Cartesian product classical waves in computing. The gate illustrated in Fig. 6 is replicated in parallel⁴³ using the lateral tunneling transistor structure. The device consists of coupled quantum structures, such as wells and wires, and an alignment gate. Without gate bias, the subband edges of

the coupled quantum wells and wires are not aligned and thus are isolated. Application of an alignment gate voltage adjusts the subband edge alignment. When the two subband edges are perfectly aligned, we can make this work as 50:50 splitter/combiner by appropriately choosing the design parameters³⁴. The device is driven by quantum physics in z direction⁴² but by classical physics in xy direction for ensemble averaging. The structure can be replicated for nonbinary weights as expected in Fig. 4. The concurrent averaging can be done by using the on-off encoding illustrated in Fig. 2 (a) such as by using $|0\rangle$ for “without electrons” and $|1\rangle$ for “with electrons.” The spatially parallel and temporarily concurrent measurement capability for the ensemble averaging is a unique capability of cubits in comparison with the measurements for qubits, which have to occur serially with no cloning. This feature should be useful in handling large fanout connections as is done by the brain. By combining blocks with this structure, a W_{ij} larger than 2×2 can be constructed. Weight update can be performed by changing the gate voltages. The effect of leakage current on the on-off ratio is a serious problem for the building blocks in classical computing but not in QIC with classical waves.

Figure 6 (d) shows integrated and fire diagram with combiner and splitter. Integrate and fire building block with combiner and splitter with quantum well and wires is shown in Fig.6 (e) with energy diagram for the integrate and fire building block in Fig. 6 (f). Details of this block has been presented elsewhere³⁴.

Appendix B: Remarks on entanglement

Finally, let us spend some time to discuss how much QIC can be closer to QC. Multiple cubit states can be represented in tensor products by using multipliers. For example, the Walsh function can be used to represent such tensor product states as those illustrated in Fig. 6. For simplicity, it is assumed that the physical pulses have square shapes in an unlimited bandwidth environment.

Entangled states such as

$$\frac{1}{\sqrt{2}}(|0\rangle|0\rangle + |1\rangle|1\rangle) \quad (36)$$

can be generated as a linear combination of the tensor product states. Since this is a local entanglement, it differs from the nonlocal entanglement in qubits. Tensor product states can be constructed in spatial degrees of freedom as well. Since the brain occupies relatively small amount of the space, this local entanglement feature can provide a similar feature with nonlocal quantum entanglement⁸. Fig. 6 shows four states, $|\alpha\rangle = |0\rangle$, $|\beta\rangle = |1\rangle$, $|\gamma\rangle = 1/\sqrt{2}(|0\rangle + |1\rangle)$, and $|\delta\rangle = 1/\sqrt{2}(-|0\rangle + |1\rangle)$, created by using the phase encoding in Fig. 2 (b), presumably with a carrier. Given these four states,

$$D(|\alpha\rangle, |\gamma\rangle) - D(|\alpha\rangle, |\delta\rangle) + D(|\beta\rangle, |\gamma\rangle) + D(|\beta\rangle, |\delta\rangle) = 2\sqrt{2}, \quad (37)$$

when $D(|x\rangle, |y\rangle) = \langle x|y\rangle$ as is commonly used in wireless coherent detection algorithms⁴⁴.

This argument may suggest that this relation is arising from wave nature, not necessarily quantum nature.

Bibliography

1. Ricciardi, L. M. and Umezawa, H. Brain and physics of many-body problems. *Kybernetik* **4** 44–48 (1967).
2. Stuart, C. I. J. Takahashi, Y. Umezawa, H. On the stability and non-local properties of memory. *J. Theor. Biol.* **71** 605–618 (1978).
3. Stuart, C. I. J. Takahashi, Y. Umezawa, H. Mixed-system brain dynamics: Neural memory as a macroscopic ordered state. *J. Found. Phys.* **9** 301–327 (1979).
4. Hameroff, S. Penrose, R. Orchestrated Objective Reduction of Quantum Coherence in Brain Microtubules: The “Orch OR2” Model for Consciousness. *Toward a Science of Consciousness - The First Tucson Discussions and Debates* MIT Press, Cambridge, MA 507–540 (1996).
5. Pribram K. H. Quantum holography: Is it relevant to brain function? *Information Sciences* **115** 97–102 (1999).
6. Alfinito, E. Vitiello, G. The dissipative quantum model of brain: How does memory localize in correlated neuronal domains. *Information Science* **128** 217–229 (2000).
7. Rebentrost, P., Mohseni, M., and Lloyd, S. Quantum support vector machine for big data classification. *Phys. Rev. Lett.* **113** 130503 (2014).
8. Biamonte, J. Quantum machine learning. *Nature* **549** 195-202 (2017).
9. Havlíček V., et al. Supervised learning with quantum-enhanced feature spaces. *Nature* **567** 209–212 (2019).
10. Grush, R. and Churchland, P. S. Gaps in Penrose’s toilings. *J. Conscious. Stud.* **2** 10–29 (1995).

11. Tegmark, M. Why the brain probably not a quantum computer. *Inform. Sci.* **128** 155–179 (2000).
12. Litt, A. *et al.* Is the Brain a Quantum Computer? *Cognitive Science* **30** 593–603 (2006).
13. Katayama, Y. Yamane, T. Nakano, D. An Energy-Efficient Computing Approach by Filling the Connectome Gap. *Unconventional Computation & Natural Computation* 229–241 (2014).
14. Katayama, Y, *et al.* Wave-Based Neuromorphic Computing Framework for Brain-Like Energy Efficiency and Integration. *IEEE Trans. Nanotechnol.* **16** 762–769 (2016).
15. Tang, E. A quantum-inspired classical algorithm for recommendation systems. *ACM STOC* (2019).
16. IBM Research Blog, AI Year in Review: Highlights of Papers and Predictions from IBM Research AI (2018) <https://www.ibm.com/blogs/research/2018/12/ai-year-review/>.
17. Preskill, J. Quantum computing and the entanglement frontier. *25th Solvay Conference* (2012).
18. Leggett, A. J. Macroscopic Quantum Systems and the Quantum Theory of Measurement. *Prog. Theor. Phys.* **69** 80–100 (1980).
19. Friedmann, J. R. *et al.* Quantum superposition of distinct macroscopic states. *Nature* **406** 43–46 (2000).
20. Feynman, R. P. Simulating physics with computers *Int. J. Theor. Phys.* **21** 467–488 (1982).
21. Bennett, C. H. Quantum information and computation. *Nature* **404** 247–255 (2000).

22. Maass, W. Networks of Spiking Neurons: The Third Generation Neural Network Models *Neural Networks* **10** 1659–1671 (1997).
23. Indiveri, G. and Liu, S.-C. Memory and information processing in neuromorphic systems *Proc. IEEE* **103** 1379–1397 (2015).
24. Merolla, P. A. *et al.* A million spiking-neuron integrated circuit with a scalable communication network and interface *Science* **345** 668–673 (2014).
25. Ambrogio, s. *et al.* Equivalent-accuracy accelerated neural-network training using analogue memory *Nature* **558** 60–67 (2018).
26. Neeley, M. Emulation of a Quantum Spin with a Superconducting Phase Qubit. *Science*, **325** 722–725 (2009).
27. Kobayashi, H. Tang, D. T. Application of Partial-Response Channel Coding to Magnetic Recording Systems. *IBM Journal of Research and Development* **14**, 368–375 (1970).
28. Fredkin, E. Toffoli, T. Conservative Logic. *Int. J. Theor. Phys.* **21** 219–253 (1982).
29. Dehaene, S. The neural basis of the Weber-Fechner law: a logarithmic mental number line. *TRENDS in Cognitive Science* **7** 145–147 (2003).
30. Singh, C, Levy, W. B. A consensus layer V pyramidal neuron can sustain interpulse-interval coding. *PLOS ONE* **12** (2017).
31. Hinton, G. E. How to do backpropagation in a brain. *NIPS Deep Learning Workshop* (2007).

32. Bengio, Y. *et al.* STDP-Compatible Approximation of Backpropagation in an Energy-Based Model. *Neural Computation* **29**, 555–577 (2017).
33. Preskill, J. Quantum computing in the NISQ era and beyond. *Quantum* **2** 79 (2018).
34. Katayama, Y. Wave-Based Spiking Neural Networks with Nano-Structured Electronics. *IEEE NANO* (2019).
35. Katayama, Y. Channel Model for Spiking Neural Networks Inspired by Impulse Radio MIMO Transmission. *IEEE GLOBECOM* to be presented (2019).
36. Bernstein, E. and Vazirani, Z. Quantum complexity theory. *SIAM J. Comput.* **26** 1411-1473 (1997).
37. Bennett C. H. The Thermodynamics of Computation – A Review. *Int. J. Theor. Phys.* **21** 905–940 (1982).
38. Singh, C and Levy, W. B. A consensus layer V pyramidal neuron can sustain interpulse-interval coding. *PLOS ONE* <https://doi.org/10.1371/journal.pone.0180839> (2017).
39. O’Keefe, J. et al., ”Place cells, navigational accuracy, and the human hippocampus”. *Philos. Trans. Royal Soc. B: Biol. Sci.* **353** 1333–1340 (1998).
40. Katayama, Y. Tsui, D. C. Lumped circuit model of two-dimensional to two-dimensional tunneling transistors. *Appl. Phys. Lett.* **62** 2563–2565 (1993).

41. Simmons, J. A. *et al.* Unipolar complementary bistable memories using gate-controlled negative differential resistance in a 2D-2D quantum tunneling transistor. *IEEE IEDM*, 755–758 (1997).
42. Katayama, Y. New Complementary Logic Circuits Using Coupled Open Quantum systems. *IEEE Trans. Nanotechnology* **4** 527–532 (2005).
43. Katayama, Y. Physical and Circuit Modeling of Coupled Open Quantum Systems. *IEEE NANO — 5th IEEE Conference on Nanotechnology* (2005).
44. Tse, D. Viswanath, P. *Fundamentals of Wireless Communication* (Cambridge University Press, 2005).

Acknowledgements The author is grateful to colleagues inside and outside IBM Research for their valuable discussions.

Competing Interests The author declares no competing interests.

Correspondence Correspondence and requests for materials should be addressed to Yasunao Katayama (email: yasunaok@jp.ibm.com).

Figure 1 Approaches for physical computing models of the brain. In the proposed approach, quantum-inspired approach for AI is investigated, ultimately aiming at unifying AI and QC computing models with classical and quantum waves.

Figure 2 Flying vs. standing cubits. Theoretically the distinction may be superficial since it is just a matter of the coordinate selection. Slower v results in smaller spatial area $v\sigma$ for each spike wave packet with the temporal width of σ and thus better integration and energy efficiency ¹⁴. The line $v = c$ represents the light cone in the Einstein-Minkowski space time. The original spatial width at standing is ignored for simplicity.

Figure 3 Physical cubit encoding examples: (a) on-off encoding, (b) phase encoding, (c) temporal encoding, (d) dual-rail encoding. To be more consistent with biological spike signaling, RZ rather than NRZ is assumed.

Figure 4 Comparison of linear and nonlinear operations for single- and multiple-input primitives in classical, quantum-inspired, and quantum computing. T represents mathematical space corresponding to the number system of choice for each basic unit.

Figure 5 Comparison of cubit and qubit operations for an artificial neuron with binary weight matrices in Cartesian and Tensor product states, respectively.

Figure 6 (a) Neural operations in QIC interpreted as ensembles of parallel and concurrent QC operations; (b) Calculated result for ensembles as a function of n_{trial} ; (c) QIC

distinguish itself from classical computing in terms of parallel execution and superposed states and from QC in terms of log-scale encoding and concurrent execution.

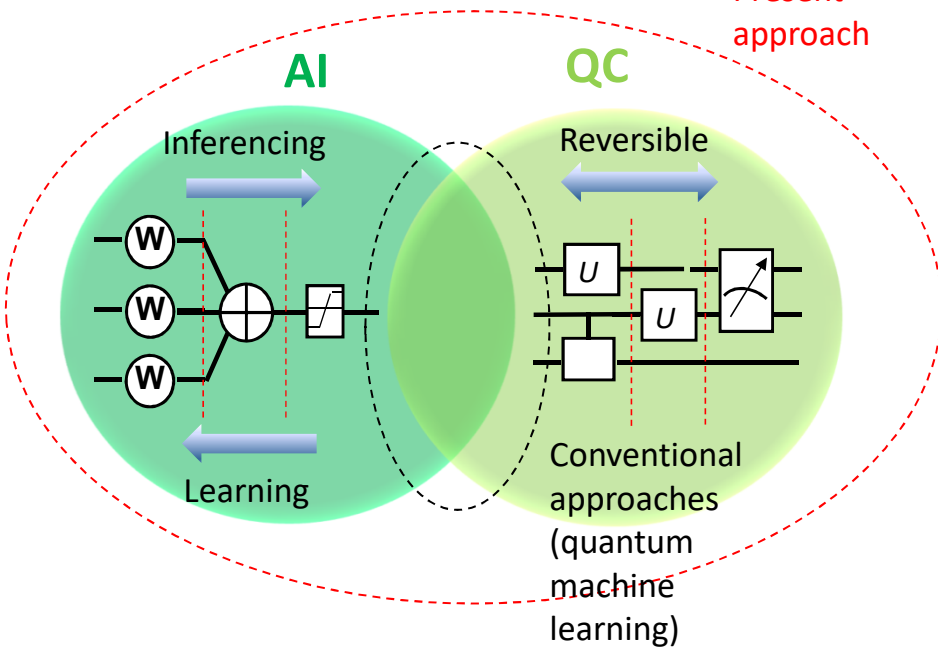
Figure 7 (a) The diagram of an example artificial neuron based on the proposed computing model; (b) Simulation results with $\Delta d = 200$ ps and 100 ps for upper and lower graphs, respectively. By appropriately adjusting the leakage time constant of the membrane potential MB, input spike temporal correlations can be extracted.

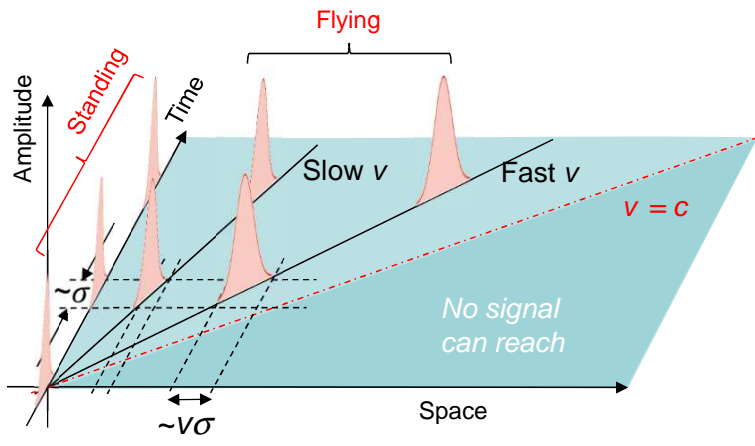
Figure 8 Implementation sketch for key primitive building blocks: (a) Weight matrix diagram represented by Fredkin gate for cubits; (b) Fredkin gate with delay for cubits with nanostructured electron wave guides and utilizes lateral tunneling transistor structure ⁴⁰; (c) Energy diagram for lateral tunneling transistor when the subband edges are misaligned and decoupled (left) and aligned and coupled (right); (d) Integrated and fire diagram with combiner and splitter; (e) Integrate and fire building block with combiner and splitter with quantum well and wires; (f) Energy diagram for the integrate and fire building block.

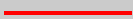
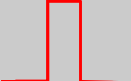
Figure 9 Cubit states are encoded into classical waves using the Walsh function. Tensor product states and local entanglement can be generated.

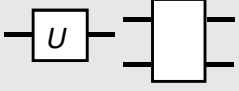
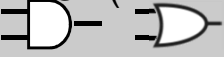
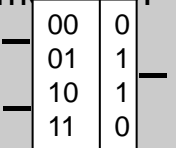
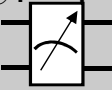
Figure 10 Coherent detection of $||\gamma\rangle\rangle$ and $||\delta\rangle\rangle$ with in-phase $||\alpha\rangle\rangle$ and quadrature $||\beta\rangle\rangle$.

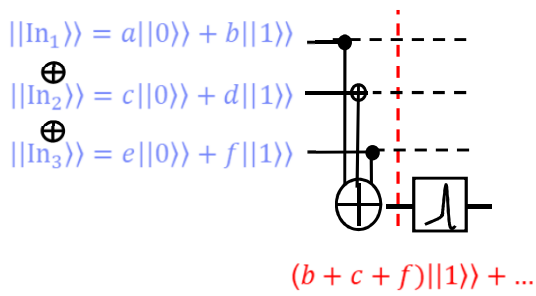
Present approach





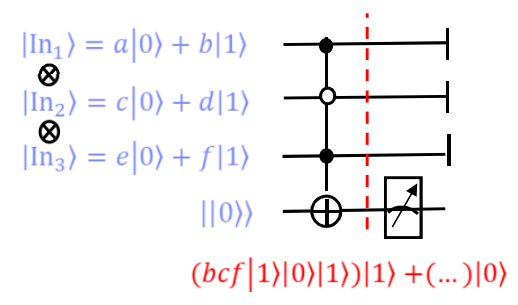
| | On-off (half cubit) | Complex phase | Temporal phase | Dual rail |
|---------------------|---|---|---|--|
| $ 0\rangle\rangle$ |  |  |  |  |
| $ 1\rangle\rangle$ |  |  |  |  |
| $ a\rangle\rangle$ |  |  |  |  |

| | Classical | Quantum-inspired | Quantum |
|----------------------|---|---|--|
| Basic unit | bit | cubit | qubit |
| Linear reversible | NOT ($T \rightarrow T$)  Fredkin/Toffoli ($T \oplus T \oplus T \rightarrow T \oplus T \oplus T$)  | Delay ($T \rightarrow T$)  Coupler ($T \oplus T \rightarrow T \oplus T$)  | All gates ($T \rightarrow T$) ($T \otimes T \rightarrow T \otimes T$) ...  |
| Linear nonreversible | XOR ($T \oplus T \rightarrow T$) (with mod 2)  | Adder/combiner/splitter ($T \oplus T \rightarrow T$)  Fixed multiplier ($T \rightarrow T$)  | |
| Nonlinear | AND/OR ($T \oplus T \rightarrow T$)  Memory ($T \oplus T \rightarrow T$)  | Multiplier ($T \otimes T \rightarrow T$)  Integrate & fire ($T \rightarrow T$)  | Measurement ($T \otimes T \rightarrow T \oplus T$)  |



$\blacklozenge W_{ij} = \begin{pmatrix} 1 & 0 \\ 0 & 1 \end{pmatrix} \quad \oplus W_{ij} = \begin{pmatrix} 0 & 1 \\ 1 & 0 \end{pmatrix} \quad + W_{ij} = \begin{pmatrix} 0 & 0 \\ 0 & 0 \end{pmatrix}$

Binary weight matrix



\blacklozenge Positive control \oplus Negative control $+$ Don't care

Quantum PNC gate

